# 2
# Flows without Particles

In this chapter, we will discuss the equations that will be solved and also the Finite Element Method formulation for flows without particles.

Newtonian incompressible flows are governed by the Navier-Stokes equations (23) that describe mass and momentum conservation. We use the hypothesis that the flow is isothermal, so that no quantity is affected by heat exchange. The equations of Mass Conservation, Eq.(2.1), and Momentum Conservation, Eq.(2.2) (23)

$$\overrightarrow{\nabla} \cdot \rho_f \overrightarrow{V} + \frac{\partial \rho_f}{\partial t} = 0 \tag{2.1}$$

$$\rho_f \left( \frac{\partial \overrightarrow{V}}{\partial t} + \overrightarrow{V} \cdot \overrightarrow{\nabla} \overrightarrow{V} \right) = \overrightarrow{\nabla} \cdot \boldsymbol{\sigma} + \rho_f \overrightarrow{g} \tag{2.2}$$

where $\overrightarrow{V}$ is the velocity vector $[u, v, w]^T$, $\rho_f$ the specific mass of the fluid, $\overrightarrow{g}$ the gravity vector $[g_x, g_y, g_z]^T$ and $\boldsymbol{\sigma}$ the incompressible Newtonian fluid stress tensor given by:

$$\boldsymbol{\sigma} = -p\boldsymbol{I} + \mu \left[ \left( \overrightarrow{\nabla} \overrightarrow{V} \right) + \left( \overrightarrow{\nabla} \overrightarrow{V} \right)^T \right] \tag{2.3}$$

Here, $p$ is the pressure, $\boldsymbol{I}$ the identity matrix and $\mu$ the fluid's dynamic viscosity.

## 2.1
## The Continuity Equation

The Continuity Equation, Eq.(2.1), assures the conservation of mass. It means that the fluid does not gain or lose mass. Mass is not created neither destroyed.

For incompressible fluids, $\rho_f$ is a constant so its derivative with respect to any quantity is zero. Thus, the continuity equation for incompressible fluids is reduced to

$$\overrightarrow{\nabla} \cdot \overrightarrow{V} = 0 \tag{2.4}$$

## 2.2
## The Momentum Conservation Equations for Newtonian Fluids

Substituting the expression for $\sigma$, Eq.(2.3), into the Momentum Conservation, Eq.(2.2), we have the Momentum Conservation for Newtonian Fluids, Eq.(2.5).

The $x$, $y$ and $z$ components of the momentum equation are presented in Appendix A.2.

$$\rho_f \overrightarrow{V} \cdot \overrightarrow{\nabla} \overrightarrow{V} = \overrightarrow{\nabla} \cdot \left\{ -p\boldsymbol{I} + \mu \left[ \left( \overrightarrow{\nabla} \overrightarrow{V} \right) + \left( \overrightarrow{\nabla} \overrightarrow{V} \right)^T \right] \right\} + \rho_f \overrightarrow{g} \tag{2.5}$$

Equations (2.4) and (2.5) constitute the strong formulation of the problem of incompressible transient flow without particles.

## 2.3 The Finite Element Method Formulation

In order to solve the system of Eqs. (2.4) and (2.5) with the Finite Element Method, we shall build the variational formulation or weak formulation.

First we shall present the interpolations made for $u$, $v$, $w$ and $p$:

$$u = \sum u_j \phi_j \tag{2.6}$$
$$v = \sum v_j \phi_j \tag{2.7}$$
$$w = \sum w_j \phi_j \tag{2.8}$$
$$p = \sum p_j \psi_j \tag{2.9}$$

where $\phi_j$ and $\psi_j$ are the basis functions used to interpolate the velocities and the pressure, respectively. In this work we chose $\phi_j$ to be tri-quadratic functions and $\psi_j$ to be piece-wise linear discontinuous. This choice of functions satisfy the Babuska-Brezzi condition (2), (3) and (4).

The weighted residue of Continuity is given by:

$$R_C^i = \int_\Omega (\nabla \cdot \overrightarrow{V}) \psi_i d\Omega \tag{2.10}$$

and the one associated with the Momentum Conservation:

$$R_m^i = \int_\Omega \rho_f \left( \overrightarrow{V} \cdot \overrightarrow{\nabla} \overrightarrow{V} - \overrightarrow{g} \right) \cdot \overrightarrow{\phi} + \sigma : \nabla \overrightarrow{\phi} \, d\Omega \tag{2.11}$$

When these residues are equal to zero, we achieved the converged solution. Once the unknown fields are substituted by their expansions as a linear combination of basis functions, a non-linear system of equations is obtained. The unknowns of the system are the coefficients of the linear expansion. Here, this system is solved by Newton's method, which requires the evaluation of the Jacobian matrix. All components of the weighted residuals and Jacobian matrix are presented in appendix A.

### 2.3.1
### The Elementary Degrees of Freedom

Each element is comprised by 27 nodes. Each node has 3 degrees of freedom (DOFs) of velocity, which are $u$, $v$ and $w$. Besides, the center node has 4 more DOFs, namely $P$, $\dfrac{\partial P}{\partial \xi}$, $\dfrac{\partial P}{\partial \eta}$, $\dfrac{\partial P}{\partial \zeta}$. All these DOFs have an elemental index. As the code was developed in C++, the indices are zero based. So the first DOF is given by index 0, the second by 1 and so on. Table 2.1 shows the indexation for each DOF of an element and fig. 2.1 shows the nodes numbering in an element.

| | | | |
|---|---|---|---|
| $0-26$ | $27-53$ | $54-80$ | $81-84$ |
| $u$ | $v$ | $w$ | $P$ |

Table 2.1: The elemental degrees of freedom and its indexation.

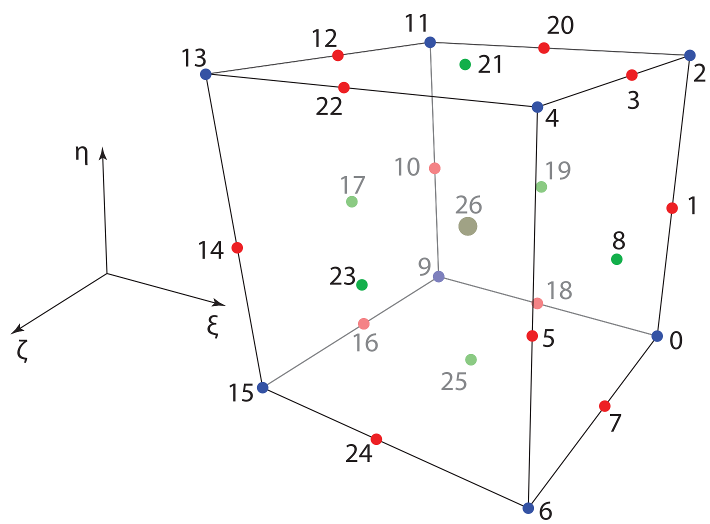


Figure 2.1: The hexahedral element, with 27 nodes. The nodes are indexed from 0 to 26.

## 2.4
## Code Validation

To validate the code, the solver was tested in steady and transient states for the lid-driven cavity flow problem in order to compare the results with the ones obtained by Lage (21). We developed a 2D code in Matlab that reproduces the results of Lage (21) and used these results to compare with our 3D code developed in C++. The Matlab code was needed because we could not run the 3D code for high Reynolds numbers.

### 2.4.1 Steady State Validation

The first test problem was a classical 2D steady state lid-driven cavity. To model this problem with the 3D code, the front and back boundaries (see fig. 2.2) were considered as simetry planes. To do so, we applied a boundary condition of no tension and $z = 0$ on these boundaries.

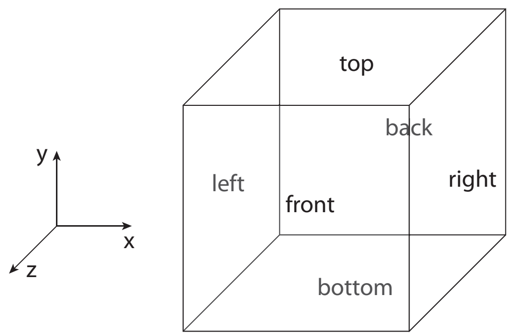


Figure 2.2: The six domain walls: front, back, left, right, bottom and top.

The top wall was set with a constant velocity of $[u_l, 0, 0]^T$ and the other three walls (left, right and bottom) were set to have zero velocity. For a lid driven cavity problem, the Reynolds number is given by equation 2.12.

$$Re = \frac{\rho_f u_l L}{\mu} \tag{2.12}$$

where $L$ is the characteristic length of the cavity and $u_l$ the lid's velocity, as seen in Figure 2.3.

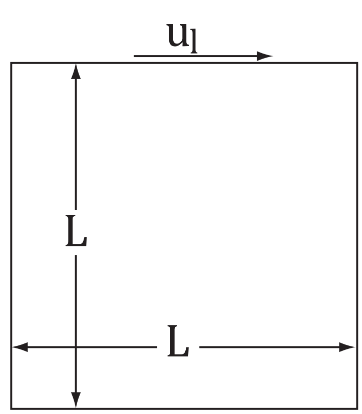


Figure 2.3: Lid-driven cavity. The cavity is a closed box with no-slip condition on the walls. The upper wall is the lid, which moves on the horizontal.

Figure 2.4 shows the velocity field plotted on the vertical plane between the front and back walls; the mesh is 25x25x1 in the 3D and 25x25 in the 2D code. The Reynolds number was set to 10. This velocity field was produced by the 3D solver and agrees with the 2D velocity field.

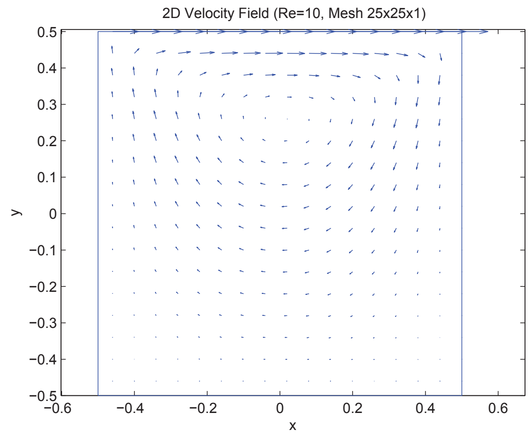


Figure 2.4: 2D velocity field generated with the 3D solver with Re=10 and a mesh of 25x25x1 elements.



Figure 2.5 displays the velocity profiles of $u$ and $v$ along the centerlines. The velocity $v$ is plotted along the horizontal centerline and the $u$ component along the vertical centerline. Both lines are on the vertical mid plane referred before. The dotted data represents the 3D results and the continuous lines the 2D.

These results agree with the ones presented by Lage (21) as expected. Lage's code is validated with results of (13).

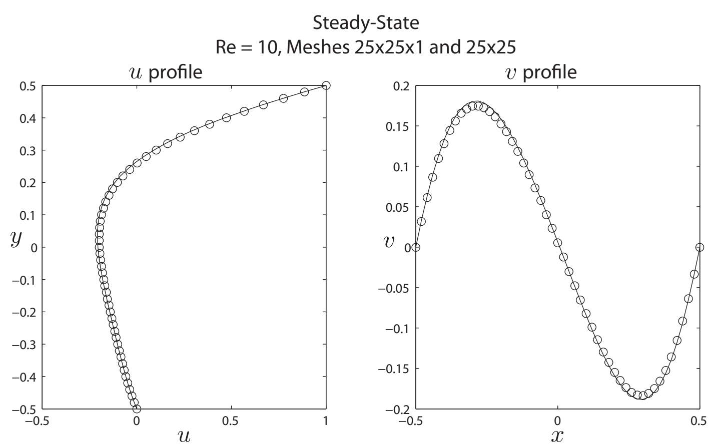


Figure 2.5: $u$ and $v$ velocities along the centerlines. Re=10 and mesh=25x25x1 elements. Circles correspond to the 3D solution and the continuous lines correspond to the 2D solution.

### 2.4.2 Transient Validation

For the transient validation, we used our 2D code already validated with the work of (21). This was necessary because our 3D code does not converge for Reynolds numbers above 60, even when using relaxation in the Newton Method. The issue is that the 3D problem generates a larger Jacobian matrix which is more ill-conditioned. We can infer that the radius of convergence of the Newton Method is not reached for high Reynolds numbers. However, we cannot measure this radius of convergence. So, we solved the transient problem for $Re = 10$ with both 2D and 3D codes and compared the results. The 2D code was ran with a 10x10 mesh and the 3D with 10x10x1. The speed of the upper wall was set to $1m/s$, $\rho_f = 10kg/m^3$ and $\mu = 1N.s/m^2$. The values agree well, as can be seen on Figures 2.6, 2.7 and 2.8. The continuous lines represent 2D data and the circles represent the 3D data.

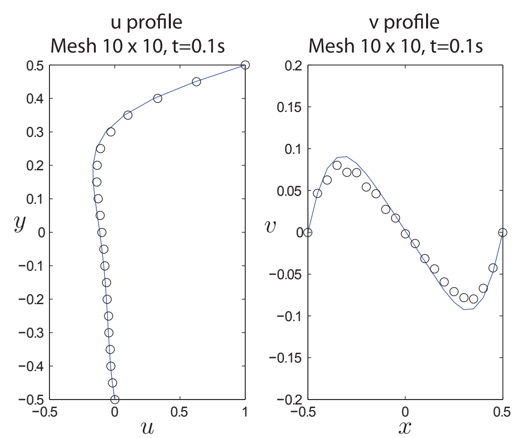


Figure 2.6: Re=10 and t=0.1s.

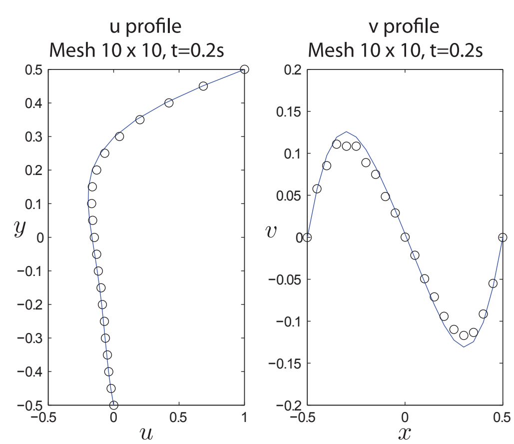


Figure 2.7: Re=10 and t=0.2s.

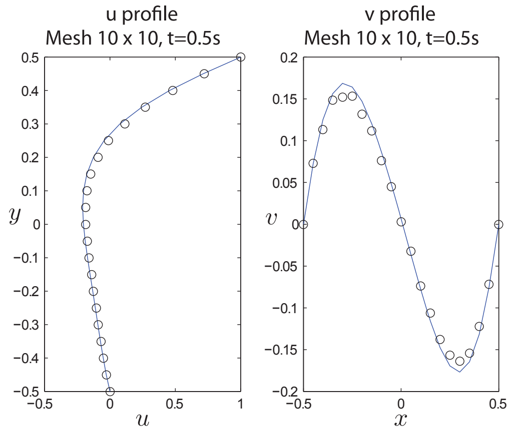


Figure 2.8: Re=10 and t=0.5s.

## 2.5 3D Transient Results

Besides the study of 2D lid-driven cavity, we also tested the solver for the 3D lid-driven cavity problem. We set the Reynolds number to 1. The velocity field on the mid vertical plane is very similar to the one of figure 2.4. The 3D velocity field can be seen in fig. 2.9. The velocity profiles on the vertical planes are similar to the 2D case, however they change in magnitude depending on the $z$ coordinate of the plane. The closer to the walls, the closer to zero they are.

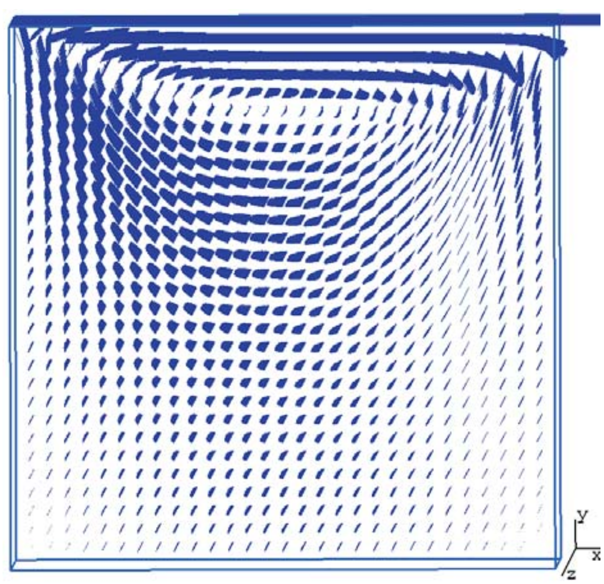


Figure 2.9: 3D velocity field of the lid-driven cavity problem.